



# Thermal shock induced dynamics of a spacecraft with a flexible deploying boom



Zhenxing Shen<sup>a,\*</sup>, Huijian Li<sup>a</sup>, Xiaoning Liu<sup>b</sup>, Gengkai Hu<sup>b</sup>

<sup>a</sup> Key Laboratory of Mechanical Reliability for Heavy Equipment and Large Structures of Hebei Province, School of Civil Engineering & Mechanics, Yanshan University, Qinhuangdao 066004, China

<sup>b</sup> Key Laboratory of Dynamics and Control of Flight Vehicle, Ministry of Education, School of Aerospace Engineering, Beijing Institute of Technology, Beijing 100081, China

## ARTICLE INFO

### Keywords:

Axially moving beam  
Thermally induced vibrations  
Absolute nodal coordinate formulation  
Rigid-flexible coupling

## ABSTRACT

The dynamics in the process of deployment of a flexible extendible boom as a deployable structure on the spacecraft is studied. For determining the thermally induced vibrations of the boom subjected to an incident solar heat flux, an axially moving thermal-dynamic beam element based on the absolute nodal coordinate formulation which is able to precisely describe the large displacement, rotation and deformation of flexible body is presented. For the elastic forces formulation of variable-length beam element, the enhanced continuum mechanics approach is adopted, which can eliminate the Poisson locking effect, and take into account the tension-bending-torsion coupling deformations. The main body of the spacecraft, modeled as a rigid body, is described using the natural coordinates method. In the derived nonlinear thermal-dynamic equations of rigid-flexible multibody system, the mass matrix is time-variant, and a pseudo damping matrix which is without actual energy dissipation, and a heat conduction matrix which is relative to the moving speed and the number of beam element are arisen. Numerical results give the dynamic and thermal responses of the nonrotating and spinning spacecraft, respectively, and show that thermal shock has a significant influence on the dynamics of spacecraft.

## 1. Introduction

The deployable booms have a wide range of applications in the space technologies, such as communication antennas, instrument carriers, and gravity gradient stabilizing [1–3]. In the course of boom deployed on orbit, the exposed part will have sudden heating changes due to the emitted thermal radiation and absorbed solar heat flux on the boom's outside surface, that is, the flexible boom is successively subjected to thermal shock during deployment. With the rapid changes of temperature gradients on the boom's cross-section, the time-dependent thermal bending moments that result in the deformations and vibrations of flexible structure are generated.

Many studies have focused on the thermally induced dynamic behaviors of deployable booms after deployment, that is, the length of boom is not changed over time. A notable example of deployable booms is STEM (Storable Tubular Extendible Member) [1], which is considered as a cantilevered beam structure and has been extensively researched by the analytical and numerical approaches. Thornton and Kim [4] derived an approximate solution for thermally induced bending vibrations of STEM as a closed thin-walled tube by means of the method of weighted

residuals, and thermal flutter phenomenon was shown in the dynamic responses. Xue et al. [5] presented a numerical approach for investigating thermally induced bending-torsion coupling vibrations of STEM as an open thin-walled tube via the finite element method. By comparing the numerical results, it is found that the temperatures and deflections responses over time are similar between the closed and open cross-section beam models. Gulick and Thornton [6], and Ko and Kim [7] studied the thermally induced vibrations of an axially spinning closed thin-walled tube by the analytical method and the finite element method, respectively. Shen and Hu [8] also studied thermally induced attitude dynamics of a spinning spacecraft with an axial boom using the absolute nodal coordinate formulation and the natural coordinates method. Above researches, the coupled thermal-structural analysis model is extensively employed, which assumes that there is an interaction effect between the absorbed solar heat flux by the tube's outside surface and the structural motions including elastic deformation and rigid rotation.

Deployable boom during deployment can be addressed as an axially moving beam. It is obviously that its dynamic analysis is more difficult than that of beam structures with constant length. A finite element method for the axially moving beam was introduced by Stylianou and

\* Corresponding author.

E-mail address: [shenzx@ysu.edu.cn](mailto:shenzx@ysu.edu.cn) (Z. Shen).

Tabarrok [9], in which the number of elements was fixed, and the size of elements is changed over time. Chang et al. [10] studied the vibration and stability based on the variable-domain element. Park et al. [11] presented a nonlinear analysis model, wherein considered the coupling effect between longitudinal and transverse vibrations of a beam with deployment and retraction. Al-Bedoor and Khulief [12], and Wang et al. [13] gave an approximate analytical solution for the free vibration of a cantilever beam with coupling of an axial translation motion and flexural deformation. Furthermore, the dynamic modeling of an axially moving beam in rotation was introduced by Yuh and Young [14], in which the approximated analytical solution was obtained by using the assumed modes method. Al-Bedoor and Khulief [15] also analyzed a beam with the rotational and translational motions, in which the softening effect due to the centripetal acceleration was included. However, the above proposed models cannot simultaneously describe the large rotation and deformation for the axially moving beam.

Thus, the absolute nodal coordinate formulation that is a non-incremental finite element method is adopted in this work. The global position and gradient vectors are selected as the nodal coordinates for modeling the rotation and deformation field of an infinitesimal volume within the element, which leads to a constant mass matrix, and eliminates the centrifugal and Coriolis inertia forces in the equations of motion [16–18]. The method has been widely used to study the dynamics of deployable space structures [19,20], and was also applied to thermally induced vibrations of flexible beam [21]. In addition, Kawaguti et al. [22] proposed a time-varying length tether element using the dimensionless variables in the frame of absolute nodal coordinate formulation. Tang et al. [23] developed also a variable-length tether element based on the absolute nodal coordinate formulation, in which the governing equations were derived by means of the hybrid Eulerian and Lagrangian framework, the arc-length coordinate of left node of tether element was a time-varying coordinate only, and the number of elements was increasing with the deployment of tether.

This paper focuses on developing an approach for determining the dynamic responses of a deployable beam structure during extension due to a sudden increase in external heating. A variable-length beam element with a constant number of elements is proposed based on the absolute nodal coordinate formulation. The coupled thermal-structural analysis model is adopted, which is to able to find the unstable dynamic response caused by thermal loading. The natural coordinates method is chosen to describe the rigid body, because of that the node coordinates are both in the global coordinate system for the absolute nodal coordinate formulation and the natural coordinates method [24]. Thermal and dynamic governing equations are solved by the weighted residual and generalized- $\alpha$  methods [25], respectively. Numerical results are conducted to

illustrate the dynamic responses of a spacecraft with a deploying boom under non-thermal loading and solar heat flux.

## 2. Modeling of the spacecraft

Consider a spacecraft composed of a rigid hub and a flexible deployable boom is subjected to solar heat flux  $S_0$ , as shown in Fig. 1.  $XYZ$  is the global coordinate system which is a fixed frame of reference, and  $xyz$  and  $\bar{x}\bar{y}\bar{z}$  are the local coordinate systems which are rigidly attached to the flexible boom and the rigid hub, respectively. The rigid-flexible structure can rotate about  $\bar{z}$ -axis with a spin rate  $\Omega$  at the initial moment, and the boom simplified as a closed thin-walled tube is deployed along its axial direction with a moving speed  $v(t)$  from the rigid hub, one end is fixed on the rigid hub, and the other is with a tip mass.

For the rigid hub described by the natural coordinates method, the position vector of one point is given by Ref. [26].

$$\bar{\mathbf{r}} = \bar{\mathbf{N}}(\bar{x}, \bar{y}, \bar{z})\bar{\mathbf{q}}(t) \tag{1}$$

where the matrix  $\bar{\mathbf{N}}$  is independent of the system's motion and therefore remains constant with time, and  $\bar{\mathbf{q}}$  is the vector of natural coordinates,

$$\bar{\mathbf{q}} = [\bar{\mathbf{r}}_i^T \quad \bar{\mathbf{r}}_j^T \quad \mathbf{u}^T \quad \mathbf{v}^T]^T \tag{2}$$

that is defined by two basic points  $i$  and  $j$ , and two unit vectors  $\mathbf{u}$  and  $\mathbf{v}$ . As shown in Fig. 1, the vectors  $\mathbf{u}$  and  $\mathbf{v}$  are parallel to  $\bar{x}$ -axis and  $\bar{y}$ -axis in the local reference frame  $\bar{x}\bar{y}\bar{z}$ , respectively.

For the flexible deployable boom modeled as an axially moving beam, the element position vector in the absolute nodal coordinate formulation of one point is proposed

$$\mathbf{r} = \mathbf{N}(x(t), y, z)\mathbf{q}(t) \tag{3}$$

where  $\mathbf{q}$  is the element nodal coordinates, for the node  $k$ , the vector of the absolute coordinates includes the position and slope vectors is defined as [16].

$$\mathbf{q}_k = \left[ \mathbf{r}_k^T \quad \frac{\partial \mathbf{r}_k^T}{\partial x} \quad \frac{\partial \mathbf{r}_k^T}{\partial y} \quad \frac{\partial \mathbf{r}_k^T}{\partial z} \right]^T \tag{4}$$

and  $\mathbf{N}$  is the element shape functions written as

$$\mathbf{N} = [N_1\mathbf{I} \quad N_2\mathbf{I} \quad \dots \quad N_8\mathbf{I}] \tag{5}$$

in which  $\mathbf{I}$  is the  $3 \times 3$  identity matrix, and the elements of matrix are

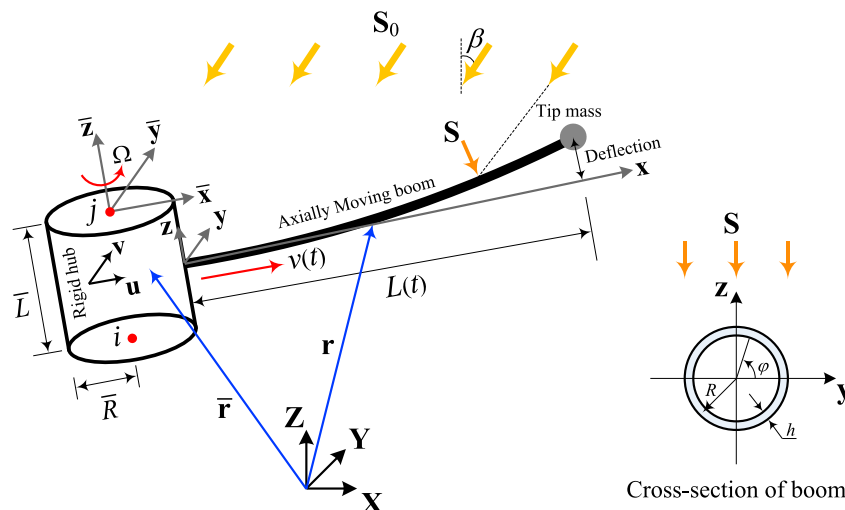


Fig. 1. Thermal-dynamic analysis model of the spacecraft with an axially moving boom.

dependent on the time  $t$ ,

$$\begin{aligned} N_1 &= 1 - 3\xi^2 + 2\xi^3, & N_5 &= 3\xi^2 - 2\xi^3, \\ N_2 &= l(t)(\xi - 2\xi^2 + \xi^3), & N_6 &= l(t)(-\xi^2 + \xi^3), \\ N_3 &= y(1 - \xi), & N_7 &= y\xi, \\ N_4 &= z(1 - \xi), & N_8 &= z\xi \end{aligned} \quad (6)$$

where  $y$  and  $z$  are the cross-section coordinates of beam,  $l$  is the element length changed with the elongating or shortening for the axially moving beam, and  $\xi$  is the axial non-dimensional coordinate,

$$\xi = \frac{x(t) - x_k(t)}{x_{k+1}(t) - x_k(t)} = \frac{x(t) - x_k(t)}{l(t)}, \quad (x_k \leq x \leq x_{k+1}) \quad (7)$$

and the axial coordinate of node  $k$  may be expressed as

$$x_k = (k - 1)l(t) = (k - 1)\frac{L(t)}{n} \quad (8)$$

where  $n$  is the number of elements, and  $L$  is the beam length in the local element coordinate system  $\mathbf{xyz}$ .

### 2.1. Thermal-dynamic equations

For the axially moving thermal-dynamic beam element, the equations of motion are derived using the D'Alembert's principle [27], which is more fundamental and applicable to variable mass systems. The virtual work of the inertia forces of an element can be represented by

$$\delta W = \int_A \int_{x_k(t)}^{x_{k+1}(t)} \rho \mathbf{r}^T \delta \mathbf{r} dx dA \quad (9)$$

in which  $A$  is the cross-section area of beam, and  $\mathbf{r}$  is the acceleration vector of a particle on the beam element obtained by differentiating Eq. (3) with respect to time  $t$ ,

$$\ddot{\mathbf{r}} = \mathbf{N}\ddot{\mathbf{q}} + 2\dot{\mathbf{N}}\dot{\mathbf{q}} + \ddot{\mathbf{N}}\mathbf{q} \quad (10)$$

where

$$\dot{\mathbf{N}} = \frac{\partial \mathbf{N}}{\partial \xi} \dot{\xi} + \frac{\partial \mathbf{N}}{\partial t} \quad (11)$$

and

$$\ddot{\mathbf{N}} = \frac{\partial^2 \mathbf{N}}{\partial \xi^2} \dot{\xi}^2 + \frac{\partial \mathbf{N}}{\partial \xi} \ddot{\xi} + 2 \frac{\partial^2 \mathbf{N}}{\partial \xi \partial t} \dot{\xi} + \frac{\partial^2 \mathbf{N}}{\partial t^2} \quad (12)$$

The rate of change with respect to time  $t$  of the element  $x$ -coordinate is given by

$$\dot{x}(t) = \dot{L}(t) = n\dot{l}(t) \quad (13)$$

The time derivatives of  $\xi$  can be then derived by using Eqs. (7), (8) and (13), one gets

$$\dot{\xi} = \frac{\dot{l}}{l}(n - j + 1 - \xi) \quad (14)$$

and

$$\ddot{\xi} = \left( \frac{\ddot{l}}{l} - 2 \frac{\dot{l}^2}{l^2} \right) (n - j + 1 - \xi) \quad (15)$$

Substituting the vectors of position and acceleration  $\mathbf{r}$  and  $\ddot{\mathbf{r}}$  into Eq. (9) yields

$$\delta W = \delta \mathbf{q}^T (\mathbf{M}_e \ddot{\mathbf{q}} + \mathbf{C}_e \dot{\mathbf{q}} + \mathbf{K}_e \mathbf{q}) \quad (16)$$

where  $\mathbf{M}_e$ ,  $\mathbf{C}_e$ , and  $\mathbf{K}_e$  are respectively the mass, pseudo damping, and

equivalent stiffness matrices of element given by

$$\mathbf{M}_e = l(t) \int_A \int_0^1 \rho \mathbf{N}^T \mathbf{N} d\xi dA \quad (17)$$

$$\mathbf{C}_e = 2l(t) \int_A \int_0^1 \rho \mathbf{N}^T \dot{\mathbf{N}} d\xi dA \quad (18)$$

$$\mathbf{K}_e = l(t) \int_A \int_0^1 \rho \mathbf{N}^T \ddot{\mathbf{N}} d\xi dA \quad (19)$$

The virtual strain energy with thermal effect of an element is derived by means of the enhanced continuum mechanics formulation [28] to remove the Poisson locking phenomenon in elastic forces formulation, which can be written as

$$\delta U = \int_A \int_{x_k(t)}^{x_{k+1}(t)} (\boldsymbol{\varepsilon} - \boldsymbol{\varepsilon}_T)^T \mathbf{D}^0 \delta(\boldsymbol{\varepsilon} - \boldsymbol{\varepsilon}_T) dx dA + A \int_{x_k(t)}^{x_{k+1}(t)} \boldsymbol{\varepsilon}^T \mathbf{D}^\nu \delta \boldsymbol{\varepsilon} dx \quad (20)$$

in which  $\boldsymbol{\varepsilon}_T$  is the thermal strain vector produced only in the first part on account of that thermal moment induces the vibrations of beam,  $\mathbf{D}^0$  and  $\mathbf{D}^\nu$  are the elasticity matrices [28], and  $\boldsymbol{\varepsilon}$  is the engineering strain vector given by

$$\boldsymbol{\varepsilon} = [\varepsilon_{xx} \quad \varepsilon_{yy} \quad \varepsilon_{zz} \quad \gamma_{xy} \quad \gamma_{yz} \quad \gamma_{zx}]^T \quad (21)$$

where the one of the normal strains may be expressed as

$$\varepsilon_{xx} = \frac{1}{2} \left( \frac{\partial \mathbf{r}^T}{\partial x} \frac{\partial \mathbf{r}}{\partial x} - 1 \right) = \frac{1}{2l(t)^2} \left( \mathbf{q}^T \frac{\partial \mathbf{N}^T}{\partial \xi} \frac{\partial \mathbf{N}}{\partial \xi} \mathbf{q} - 1 \right) \quad (22)$$

and the one of the shear strains is

$$\gamma_{xy} = \frac{\partial \mathbf{r}^T}{\partial x} \frac{\partial \mathbf{r}}{\partial y} = \frac{1}{l(t)} \mathbf{q}^T \frac{\partial \mathbf{N}^T}{\partial \xi} \frac{\partial \mathbf{N}}{\partial y} \mathbf{q} \quad (23)$$

Similarly, the expression for the other normal and shear strains can be also obtained. Thermal strain vector after ignoring thermally induced transverse deformations can be written as

$$\boldsymbol{\varepsilon}_T = [\alpha_T(T - T_0) \quad 0 \quad 0 \quad 0 \quad 0 \quad 0]^T \quad (24)$$

where  $\alpha_T$  is the coefficient of thermal expansion,  $T_0$  is the reference temperature, and the temperature  $T$  is related to the structural deformations, and can be obtained by thermal analysis in the following section. Substituting Eqs. (21)–(24) into Eq. (20) leads to

$$\delta U = \delta \mathbf{q}^T (\mathbf{Q}^0 + \mathbf{Q}^\nu - \mathbf{Q}_T) \quad (25)$$

where  $\mathbf{Q}$  are the element elastic forces composed by three parts, in which  $\mathbf{Q}^\nu$  considers the Poisson effect at the beam axis,  $\mathbf{Q}^0$  neglects the effect, and  $\mathbf{Q}_T$  is produced by the gradient distribution of temperature on the beam cross-section. Their expressions are written respectively as

$$\mathbf{Q}^0 = l(t) \int_A \int_0^1 \sum_{i=1}^6 (\mathbf{D}^0 \boldsymbol{\varepsilon})_i \frac{\partial \varepsilon_i}{\partial \mathbf{q}} d\xi dA \quad (26)$$

$$\mathbf{Q}^\nu = l(t) A \int_0^1 \sum_{i=1}^3 (\mathbf{D}^\nu \boldsymbol{\varepsilon})_i \frac{\partial \varepsilon_i}{\partial \mathbf{q}} d\xi \quad (27)$$

$$\mathbf{Q}_T = l(t) \int_A \int_0^1 E \alpha_T (T - T_0) \frac{\partial \varepsilon_{xx}}{\partial \mathbf{q}} d\xi dA \quad (28)$$

where  $\varepsilon_i$  is the  $i$ th element of vector  $\boldsymbol{\varepsilon}$ , and  $E$  is the Young's modulus.

For the rigid hub, the mass matrix can be derived by means of the position vector in Eq. (1) and the virtual work of the inertia forces [26], and follows to

$$\bar{\mathbf{M}} = \bar{m} \begin{bmatrix} \frac{1}{3}\mathbf{I} & \frac{1}{6}\mathbf{I} & \mathbf{0} & \mathbf{0} \\ \frac{1}{6}\mathbf{I} & \frac{1}{3}\mathbf{I} & \mathbf{0} & \mathbf{0} \\ \mathbf{0} & \mathbf{0} & \frac{\bar{R}^2}{4}\mathbf{I} & \mathbf{0} \\ \mathbf{0} & \mathbf{0} & \mathbf{0} & \frac{\bar{R}^2}{4}\mathbf{I} \end{bmatrix} \quad (29)$$

where  $\bar{m}$  and  $\bar{R}$  are the mass and radius of rigid hub, and  $\mathbf{I}$  and  $\mathbf{0}$  are  $3 \times 3$  identity and null matrices, respectively.

For the spacecraft as a rigid-flexible multibody system, the rigid joint between the axially moving beam and the rigid hub is defined by the constraint equations, one can write

$$\bar{\Phi} = \begin{bmatrix} \mathbf{r}_1 - \frac{\mathbf{r}_i + \mathbf{r}_j}{2} - \bar{R}\mathbf{u} \\ \frac{\partial \mathbf{r}_1^\top}{\partial x} (\mathbf{r}_j - \mathbf{r}_i) \\ \frac{\partial \mathbf{r}_1^\top}{\partial y} (\mathbf{r}_j - \mathbf{r}_i) \\ \frac{\partial \mathbf{r}_1^\top}{\partial x} \mathbf{v} \end{bmatrix} = \mathbf{0} \quad (30)$$

where the subscript 1 denotes the first node of beam, that is,  $k = 1$ . And the thermal-dynamic equations that along with the associated constraint equations are given by

$$\left\{ \mathbf{M}(\mathbf{t})\ddot{\mathbf{e}} + \mathbf{C}(\mathbf{t})\dot{\mathbf{e}} + \mathbf{K}(\mathbf{t})\mathbf{e} + \mathbf{Q}(\mathbf{e}, \mathbf{t}) + \Phi_e^\top(\mathbf{e})\lambda = \mathbf{0} \quad \Phi(\mathbf{e}) = \mathbf{0} \quad (31) \right.$$

where  $\mathbf{e}$  is the total vector of generalized coordinates which includes  $\bar{\mathbf{q}}$  and  $\mathbf{q}$ ,  $\mathbf{M}$  is the global mass matrix composed by  $\bar{\mathbf{M}}$  and the assembly of  $\mathbf{M}_e$ , and  $\mathbf{C}$ ,  $\mathbf{K}$ , and  $\mathbf{Q}$  are respectively the assembly of element matrices  $\mathbf{C}_e$ ,  $\mathbf{K}_e$ , and the element elastic forces in Eq. (25),  $\Phi$  is the constraint equations which contains  $\Phi$  and the rigid body constraints [26],  $\Phi_e$  is the Jacobian of constraint, and  $\lambda$  is the Lagrange multipliers [27]. The system of Eq. (31) is a set of nonlinear differential-algebraic equations with varying-time coefficients, which may be solved by the generalized- $\alpha$  method [25].

### 2.2. Thermal analysis of boom

The axially moving boom modeled as a closed thin-walled tube, is subjected to thermal shocking during deployment because of an incident solar heat flux  $\mathbf{S}_0$ . Using the coupled thermal-structural analysis model, the heat conduction equation of tube can be derived based on the principle of conservation of energy and the assumptions given in Ref. [29], one gets

$$\rho c \frac{\partial T}{\partial t} - k_x \frac{\partial^2 T}{\partial x^2} - \frac{k_\varphi}{R^2} \frac{\partial^2 T}{\partial \varphi^2} + \frac{\sigma_T \varepsilon_T}{h} (T^4 - T_\infty^4) = \frac{\alpha_s S}{h} \delta \sin \varphi \quad (32)$$

where  $\rho$  is the mass density,  $c$  is the specific heat,  $k_x$  and  $k_\varphi$  are respectively the thermal conductivity along the axial and circumferential directions,  $R$  and  $h$  shown in Fig. 1 are respectively the radius and wall thickness of tube,  $\sigma_T$  is the Stefan-Boltzmann constant,  $\varepsilon_T$  is the emissivity,  $T_\infty$  is the surrounding temperature that is assumed to be 0 K,  $\alpha_s$  is the absorptivity, and  $S$  is the norm of the projected solar heat flux  $\mathbf{S}$  shown in Fig. 1, which is dependent of the structural deformations and motions, and can be obtained by

$$S = -\mathbf{S}_0 \cdot \frac{\mathbf{r}_z}{|\mathbf{r}_z|} \quad (33)$$

where  $\mathbf{r}_z$  is the slope vector along  $z$ -direction on the beam cross section, and the parameter  $\delta$  is given by

$$\delta = \begin{cases} 1, & 0 < \varphi < \pi \\ 0, & -\pi \leq \varphi \leq 0 \end{cases} \quad (34)$$

that is, the upper part of the tube's outside surface is heated when  $\delta$  is the unity, as shown in Fig. 1.

To solve Eq. (32), the term including  $\delta$  is considered by Fourier series expanded technique, which is expressed as [8].

$$\delta \sin \varphi \approx \frac{1}{\pi} + \frac{1}{2} \sin \varphi \quad (35)$$

and the temperature distributions along the circumferential and axial directions are approximated by means of the trigonometric functions and the linear interpolation functions, respectively. The temperature of an arbitrary point on the beam element can then be written as [8].

$$T = [1 - \xi \quad \xi] \begin{bmatrix} T_k^{(0)} + T_k^{(1)} \sin \varphi + T_k^{(2)} \cos \varphi \\ T_{k+1}^{(0)} + T_{k+1}^{(1)} \sin \varphi + T_{k+1}^{(2)} \cos \varphi \end{bmatrix} \quad (36)$$

where  $\xi$  is the axial non-dimensional coordinate given in Eq. (7),  $k$  is the node number,  $T^{(0)}$  is defined as the average temperature, and  $T^{(1)}$  and  $T^{(2)}$  are the perturbation temperatures.

Substituting Eqs. (35) and (36) into Eq. (32), then decoupling the obtained equation by means of the weighted residual method, and using  $1-\xi$  and  $\xi$  as the weight functions, respectively, one can obtain the element equations in a matrix form of the average temperatures,

$$\mathbf{C}_T \dot{\mathbf{T}}^{(0)} + [\mathbf{K}_x(\mathbf{t}) + \mathbf{K}_c(\mathbf{t}) + \mathbf{K}_r(\mathbf{T}^{(0)})] \mathbf{T}^{(0)} = \mathbf{R}_T(\mathbf{q}) \quad (37)$$

where the constant coefficient  $\mathbf{C}_T$  is the element capacitance matrix, the

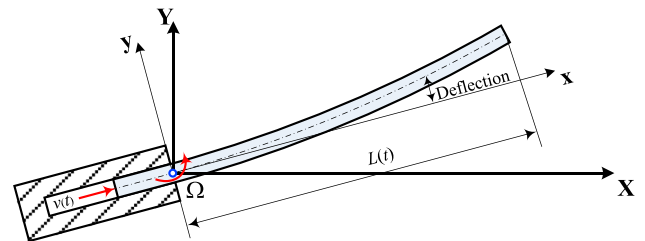


Fig. 2. The axially moving beam in rotation.

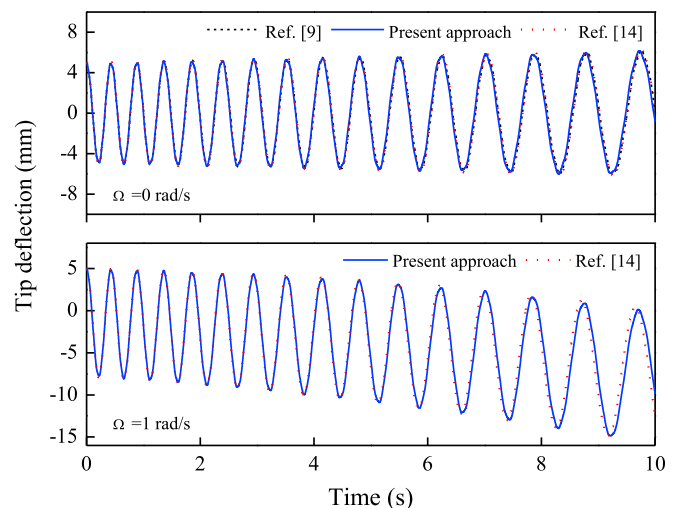


Fig. 3. Comparison of tip deflection history for the axially moving beam without rotation and in constant rotating speed.

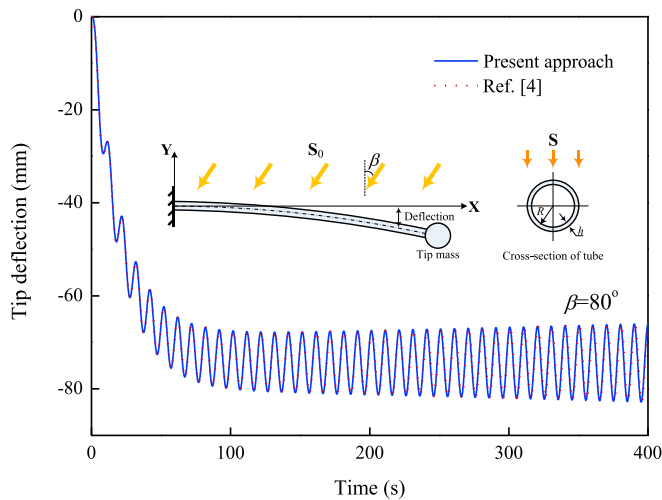


Fig. 4. Comparison of tip deflection history for a cantilevered and non-moving beam under the solar heat flux.

Table 1  
Thermal-structural data for thin-walled tube.

Parameter	Value	Units
$R$	$9.53 \times 10^{-3}$	m
$h$	$2.03 \times 10^{-4}$	m
$E$	152.18	GPa
$\nu$	0.3	–
$\rho$	8026	kg/m <sup>3</sup>
$c$	502	J/kg.K
$k_x$	16.6	W/m.K
$k_\varphi$	16.6	W/m.K
$\alpha_s$	0.5	–
$\alpha_T$	$1.69 \times 10^{-5}$	1/K
$\varepsilon_T$	0.13	–
$S_0$	1350	W/m <sup>2</sup>

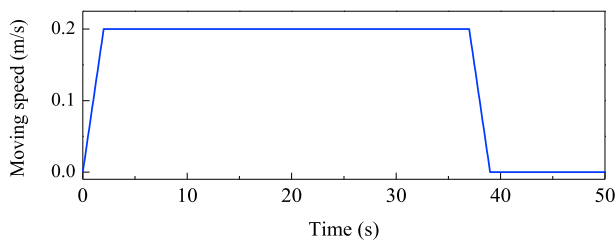


Fig. 5. Deploying speed profile of the axially moving boom.

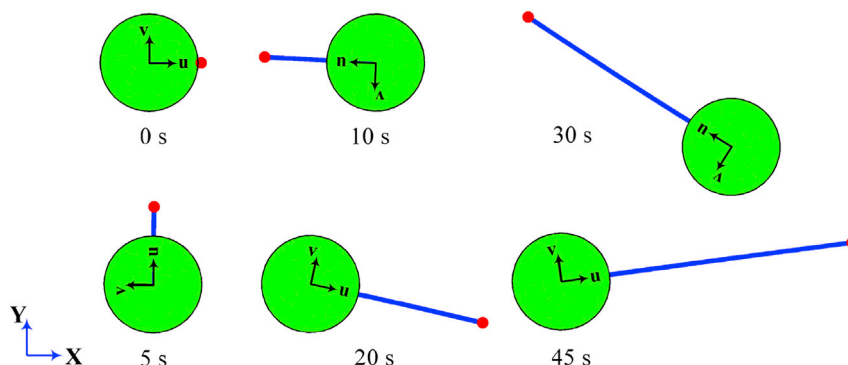


Fig. 6. Configuration of the spacecraft with a spin rate 3 rpm at certain times.

time-dependent coefficients  $K_x$  and  $K_c$  are the element conductance matrices related to heat conduction along the axial direction, the temperature-dependent coefficient  $K_r$  is generated by radiation heat transfer [30], and the vector  $R_T$  that is related to the structural deformations and motions is the heat loading due to the solar heat flux, which are, respectively, given by

$$C_T = \frac{\rho c}{6} \begin{bmatrix} 2 & 1 \\ 1 & 2 \end{bmatrix}, \quad K_x = \frac{k_x}{l(t)^2} \begin{bmatrix} 1 & -1 \\ -1 & 1 \end{bmatrix}, \quad (38)$$

$$K_c = \frac{\rho c}{6} \frac{\dot{l}(t)}{l(t)} \begin{bmatrix} -3n + 3k - 2 & 3n - 3k + 2 \\ -3n + 3k - 1 & 3n - 3k + 1 \end{bmatrix}, \quad (39)$$

$$K_r = \frac{\sigma_T \varepsilon_T}{2h} \begin{bmatrix} T_k^{(0)3} & 0 \\ 0 & T_{k+1}^{(0)3} \end{bmatrix}, \quad R_T = \frac{\alpha_s S}{2\pi h} \begin{bmatrix} 1 \\ 1 \end{bmatrix} \quad (40)$$

It should be noted that  $K_c$  involves the axially moving speed and the node number. Using  $(1-\xi) \sin\varphi$ ,  $\xi \sin\varphi$ ,  $(1-\xi) \cos\varphi$ , and  $\xi \cos\varphi$  as the weight functions, respectively, one obtains

$$C_T \dot{T}^{(1)} + (K_x + K_c + K_\varphi + 4K_r) T^{(1)} = \frac{\pi}{2} R_T \quad (41)$$

$$C_T \dot{T}^{(2)} + (K_x + K_c + K_\varphi + 4K_r) T^{(2)} = 0 \quad (42)$$

where the constant coefficient  $K_\varphi$  is the element conductance matrix related to heat conduction along the circumferential direction,

$$K_\varphi = \frac{k_\varphi}{6R^2} \begin{bmatrix} 2 & 1 \\ 1 & 2 \end{bmatrix} \quad (43)$$

The boundary conditions of boom are the constant temperature 290 K and the heat insulation at the rigid joint and the tip mass, respectively. Finally, Eq. (37) as a set of non-linear equations can be solved by means of the Wilson- $\theta$  method together with the Newton-Raphson iteration [30]. The perturbation temperatures  $T^{(1)}$  in Eq. (41) are then calculated by substituting the obtained average temperatures  $T^{(0)}$  into the element matrix  $K_r$ , and the perturbation temperatures  $T^{(2)}$  are not evaluated due to no thermal loading in Eq. (42). Especially, the thermal-dynamic coupling analysis is performed by solving interactively Eqs. (31), (37) and (41) in each time step.

### 3. Validation

In order to validate the proposed beam element without thermal effect, a classical dynamics analysis for an axially moving beam shown in Fig. 2 is firstly considered. The beam has the mass density  $\rho = 2738.6$  kg/m<sup>3</sup>, Young's modulus  $E = 68.335$  GPa, cross-sectional area  $A = 1.4661 \times 10^{-3}$  m<sup>2</sup>, area moment of inertia  $I = 1.1073 \times 10^{-8}$  m<sup>4</sup>, and a constant moving speed 0.1 m/s. At the initial time, the beam length

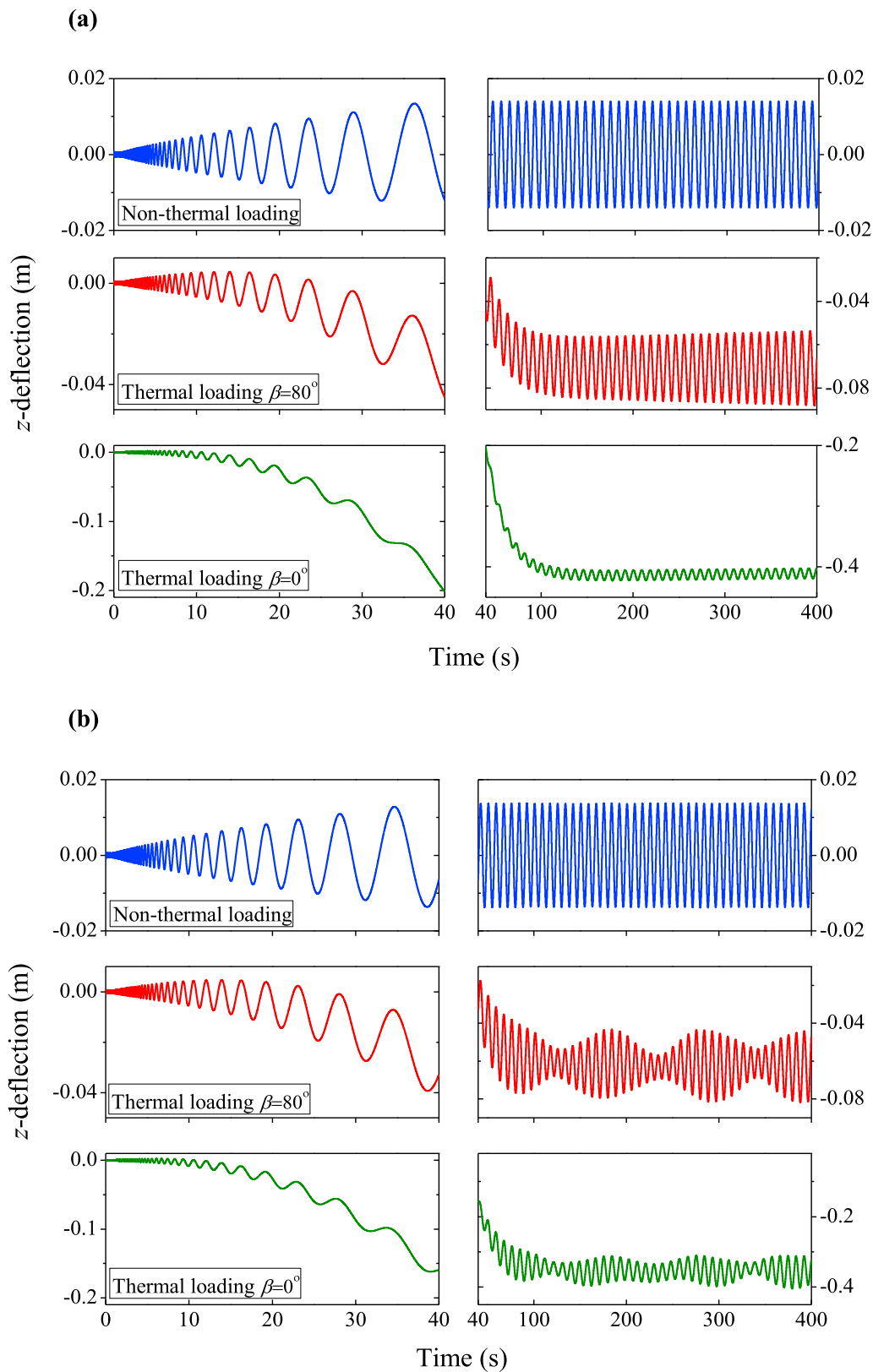


Fig. 7. Tip z-deflection history of the axially moving boom. (a)  $\Omega=0$  rpm; (b)  $\Omega=3$  rpm.

is 1.8 m, and the deflection at the tip is 5 mm. Fig. 3 shows the tip deflections over time for the beam without and in rotation, respectively. The results obtained by the present approach using 10 beam elements agree well with the methods in references.

To verify the presented thermal-dynamic analysis, another

comparison is shown in Fig. 4. The beam is a cantilevered and non-moving tube structure, and subjected to solar heat flux. It has the length 7.5 m, the initial temperature 290 K, and the tip mass 1.5 kg. And the other properties are listed in Table 1, where  $\nu$  is the Poisson's ratio, and  $S_0$  is the norm of solar heat flux  $S_0$ . As shown in Fig. 4, the response

computed by the present approach using 10 beam elements is nearly the same as that obtained by means of the analytical method in Ref. [4].

#### 4. Numerical results

In this section, dynamic and thermal responses for the spacecraft shown in Fig. 1, are presented to illustrate thermally induced dynamics of a flexible deploying boom under the solar heat flux. For the rigid hub, the height  $\bar{L}$  is 2 m, the radius  $\bar{R}$  is 1.5 m, and the mass  $\bar{m}$  is 500 kg. For the axially moving boom, the initial length is 0.1 m, the initial tip  $z$ -deflection is 1 mm, the initial temperature is 290 K, the tip mass is 1.5 kg, and the other properties are given in Table 1. In addition, the moving speed  $v(t)$  is shown in Fig. 5, the boom's length  $L(t)$  can then be obtained by integrating the moving speed, and the boom length after deployment is 7.5 m. As shown in Fig. 5, the deploying boom has a constant acceleration 0.1 m/s<sup>2</sup> for  $0 \leq t \leq 2$  s, a constant velocity 0.2 m/s for  $2 \leq t \leq 37$  s, a constant acceleration  $-0.1$  m/s<sup>2</sup> for  $37 \leq t \leq 39$  s, and a constant velocity 0 m/s for  $t \geq 39$  s, that is, the deployment is stopped at 39 s.

The configuration at certain times for the spinning spacecraft with a flexible deploying boom without thermal loading is shown firstly in Fig. 6, in which the spin rate 3 rpm is applied on the spacecraft at the initial moment. In order to illustrate the influence of the rigid hub rotation to dynamic responses, the non-spinning spacecraft ( $\Omega = 0$  rpm) is also considered in the following. The deflection responses of the flexible boom are described in the body coordinate system  $xyz$ , which can be calculated by the transformation matrix between the local and global components defined as

$$\mathbf{A} = [\mathbf{u} \quad \mathbf{v} \quad (\bar{\mathbf{r}}_j - \bar{\mathbf{r}}_i)/\bar{L}] \quad (44)$$

Fig. 7 shows the transverse vibration on  $z$ -direction of the boom during and after deployment. It can be seen that the thermal loading has a significant influence on the vibration responses, and the difference is more and more obvious as the increasing of thermal loading. That is because there is the thermal moment at the cross-section when the boom is subjected to solar heat flux, which is related to the thermal elastic force in Eq. (28). For the dynamic responses during deployment, the vibrations are generated due to the small deflection at the initial moment, the amplitude and the frequency are increased and decreased respectively with the increasing of the boom's length, and there is no significant difference between  $\Omega = 0$  rpm and  $\Omega = 3$  rpm. For the dynamic responses after deployment, the thermal flutter [1] is still demonstrated in Fig. 7(a) for  $\beta = 80^\circ$ , which is similar to the results in Fig. 4, and can be obtained only by the coupled thermal-structural analysis. The beat phenomenon induced by the spin of spacecraft is also found in Fig. 7(b), but the phenomenon is not obvious for the non-thermal loading.

Fig. 8 shows only the transverse vibration on  $y$ -direction for the boom in rotation, because there is no  $y$ -deflection for the boom on non-spinning spacecraft. In addition, the response for thermal loading  $\beta = 0^\circ$  is shown

only due to that there is almost no difference between  $\beta = 80^\circ$  and  $\beta = 0^\circ$ . And there is no significant difference between the results with and without thermal loading, due to that the boom's deformations induced by the solar heat flux is only on the  $z$ -direction. In addition, there is no  $y$ -deflection at the initial moment, thus the vibration responses during deployment are caused by the rotation of rigid hub and the deployment of flexible boom.

Fig. 9 shows the attitude angle of the rigid hub, which is evaluated by the include angle between  $\bar{z}$ -axis and  $Z$ -axis. For the non-spinning spacecraft ( $\Omega = 0$  rpm), a sign convention is established so as to define positive and negative values for the attitude angle. The positive value is that the angle is counterclockwise from  $Z$ -axis to  $\bar{z}$ -axis in  $X$ - $Z$  plane. The direction that is opposite to it is considered negative. However, for the spinning spacecraft, three coordinate direction angles are needed to determine its attitude, which results in that the above sign convention cannot be used. The attitude responses of rigid hub are caused by the change of boom length and thermal elastic force. It is also obvious that the thermal loading has a significant influence on the attitude dynamics of spacecraft. For the attitude angle during the deployment of boom, the amplitude of oscillation is remained increase over time. In addition, the response shape in Fig. 9(a) is similar to that of  $z$ -deflection in Fig. 7(a), and the beat phenomenon is also shown for the spinning spacecraft in Fig. 9(b). Specially, the amplitude of attitude angle is not decreased with the rotation of rigid hub by comparing these results between Fig. 9(a) and (b).

Fig. 10 shows the thermal responses of average temperature  $T^{(0)}$  and perturbation temperature  $T^{(1)}$  for some certain point on the axially moving boom without rotation. The average temperature in Fig. 10(a) is decreased gradually with increase of time, on the contrary in Fig. 10(b). That is because the absorbed solar heat flux is less than the radiated thermal energy through the outside surface of boom for the  $80^\circ$  solar incident angle. However, the perturbation temperatures that cause the thermal bending deformations are both increased over time. In addition, the perturbation temperature for  $\beta = 80^\circ$ , as shown in Fig. 10(c), has a small oscillation, which results in the thermal flutter phenomenon shown in Fig. 7(a). For the response shape of node 3, there is obviously an inflection point, which is due to that the node 1 temperature is fixed at 290 K, and the distance between node 1 and node 3 is relatively near.

#### 5. Conclusions

A new thermal-dynamic finite element in the frame of absolute nodal coordinate formulation is developed for determining the thermally induced dynamics of a spacecraft with the flexible deploying boom subjected to a sudden solar heating. The longitudinal and transverse vibrations of an axially moving beam in large rotations and deformations can be analyzed by means of the proposed element. In the equations of motion, the mass, damping, and stiffness matrixes are all dependent of time, and the coupling between rigid hub and flexible boom may be

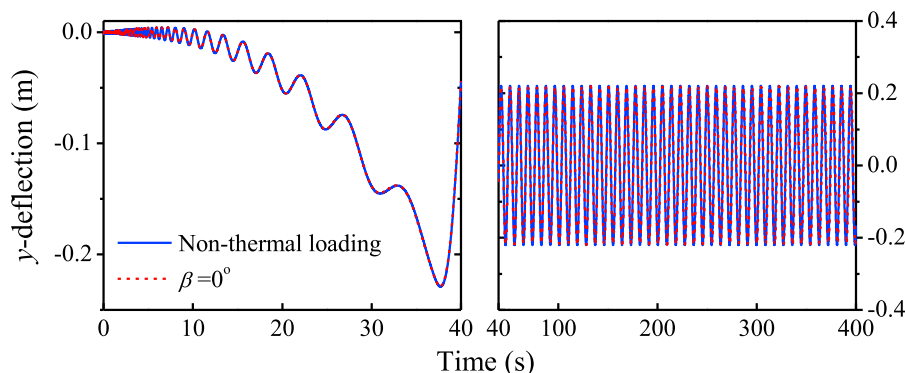


Fig. 8. Tip  $y$ -deflection history of the axially moving boom for  $\Omega = 3$  rpm.

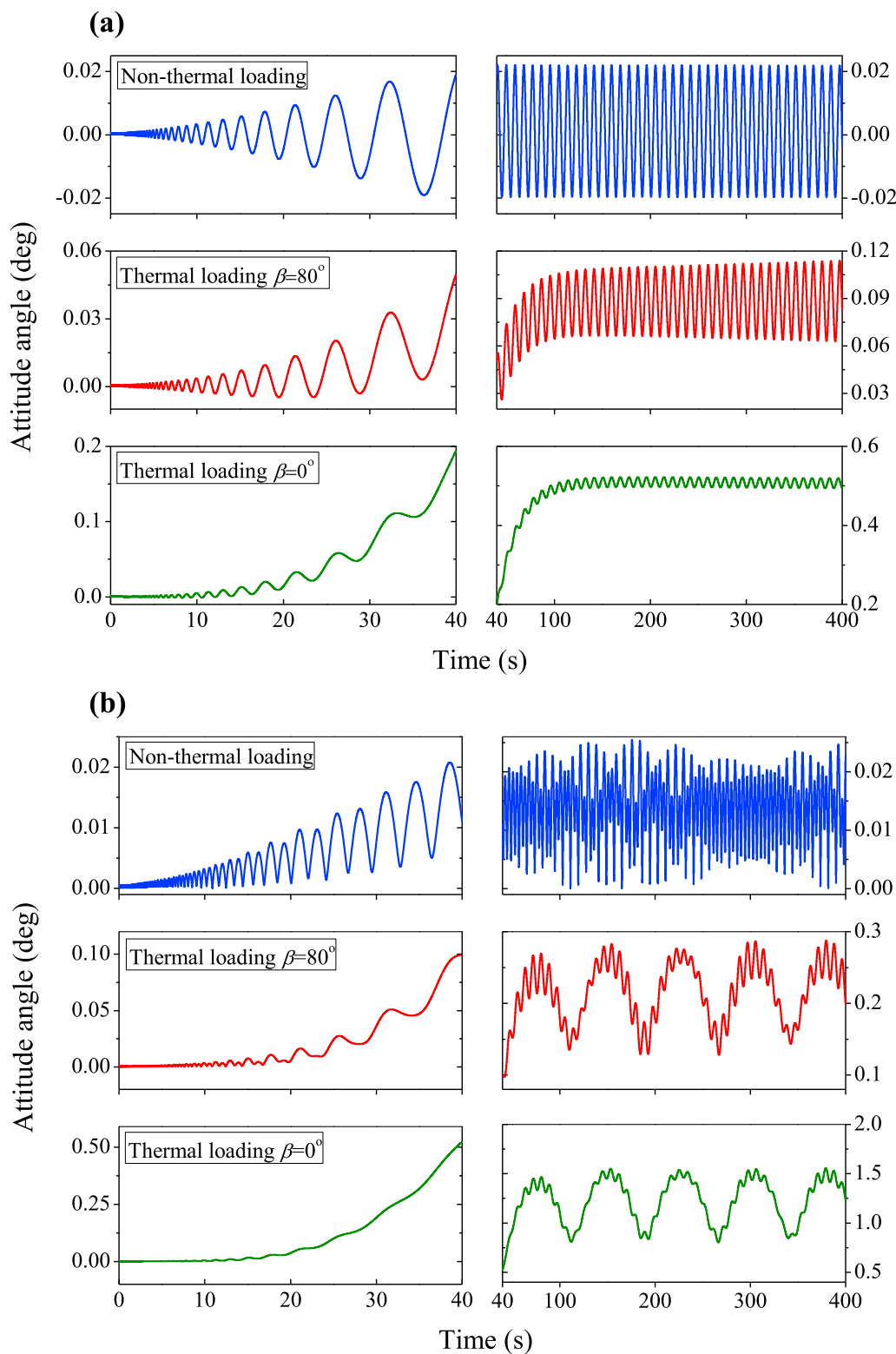


Fig. 9. Attitude angle history of the rigid hub. (a)  $\Omega=0$  rpm; (b)  $\Omega=3$  rpm.

easily achieved by the constraint equations. The present approach shows a good performance by comparing the results with references.

Through the numerical results, it is found that the thermal loading has a significant influence on the dynamic responses, and the amplitude and frequency of dynamic response are respectively increased and decreased with the deployment of boom. Thermal flutter is still shown for the large

solar incident angle by means of the coupled thermal-structural analysis model. The beat phenomenon is obvious when the spinning spacecraft subjected to thermal shock. In addition, there is a significant difference between the nonrotating and spinning spacecraft for the dynamic responses after the deployment of boom.

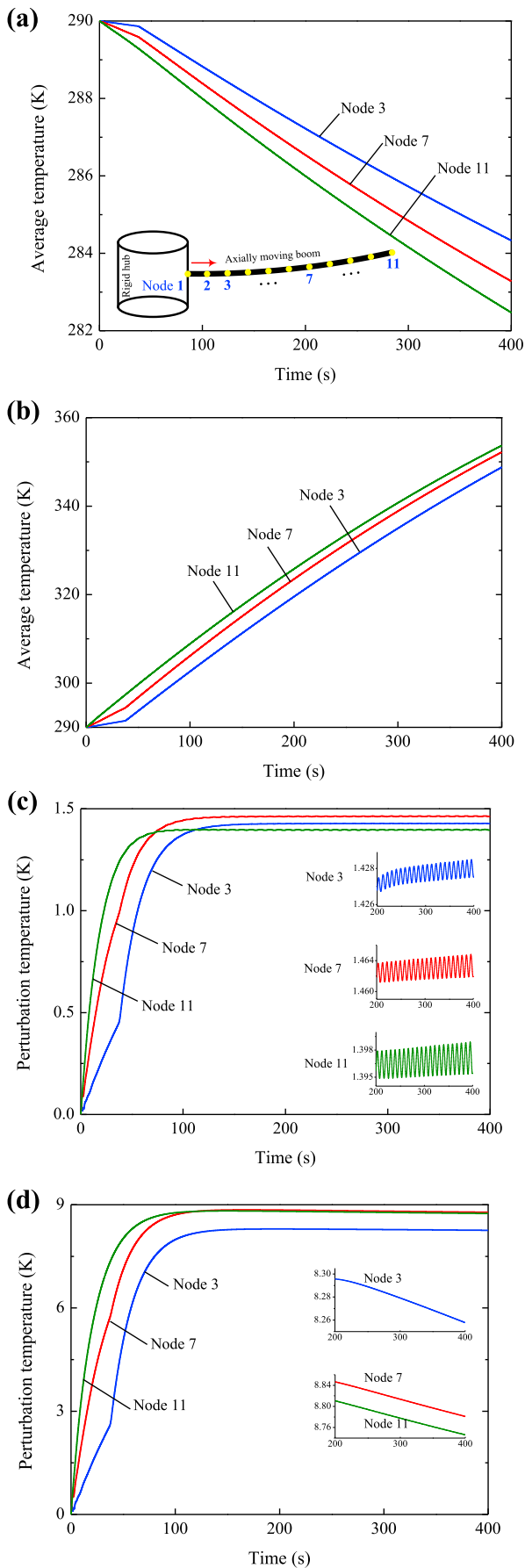


Fig. 10. Average and perturbation temperatures history of the axially moving boom. (a)  $\beta=80^\circ$ ; (b)  $\beta=0^\circ$ ; (c)  $\beta=80^\circ$ ; (d)  $\beta=0^\circ$ .

### Acknowledgment

This work was supported by the National Natural Science Foundation of China under Grants 11702241, 11290152 and 11521062, the Natural Science Foundation of Hebei Province of China under Grant A2017203272, and the Science and Technology Research Program in Higher Education of Hebei Province of China under Grant QN2017149.

### References

- [1] E.A. Thornton, R.S. Foster, Dynamic response of rapidly heated space structures, in: 33rd Structures, Structural Dynamics and Materials Conference, 1992.
- [2] V.I. Dranovskii, V.S. Khoroshylov, A.E. Zakrzhevskii, Spacecraft dynamics with regard to elastic gravitational stabilizer deployment, *Acta Astronaut.* 64 (2009) 501–513.
- [3] P. Mallol, G. Tibert, Deployment modeling and experimental testing of a bi-stable composite boom for small satellite, in: 54th AIAA/ASME/ASCE/AHS/ASC Structures, Structural Dynamics, and Materials Conference, 2013.
- [4] E.A. Thornton, Y.A. Kim, Thermally-induced bending vibrations of a flexible rolled-up solar-array, *J. Spacecr. Rockets* 30 (4) (1993) 438–448.
- [5] M.D. Xue, J. Duan, Z.H. Xiang, Thermally-induced bending-torsion coupling vibration of large scale space structures, *Comput. Mech.* 40 (4) (2007) 707–723.
- [6] D.W. Gulick, E.A. Thornton, Thermally-induced vibrations of a spinning spacecraft boom, *Acta Astronaut.* 36 (3) (1995) 163–176.
- [7] K.E. Ko, J.H. Kim, Thermally induced vibrations of spinning thin-walled composite beam, *AIAA J.* 41 (2) (2003) 296–303.
- [8] Z. Shen, G. Hu, Thermally induced dynamics of a spinning spacecraft with an axial flexible boom, *J. Spacecr. Rockets* 52 (5) (2015) 1503–1508.
- [9] M. Stylianou, B. Tabarrok, Finite element analysis of an axially moving beam, part I: time integration, *J. Sound. Vib.* 178 (4) (1994) 433–453.
- [10] J.R. Chang, W.J. Lin, C.J. Huang, S.T. Choi, Vibration and stability of an axially moving Rayleigh beam, *Appl. Math. Model* 34 (6) (2010) 1482–1497.
- [11] S. Park, H.H. Yoo, J. Chung, Vibrations of an axially moving beam with deployment or retraction, *AIAA J.* 51 (3) (2013) 686–696.
- [12] B.O. Al-Bedoor, Y.A. Khulief, An approximate analytical solution of beam vibrations during axial motion, *J. Sound. Vib.* 192 (1) (1996) 159–171.
- [13] L.H. Wang, Z.D. Hu, Z. Zhong, J.W. Ju, Hamiltonian dynamic analysis of an axially translating beam featuring time-variant velocity, *Acta Mech.* 206 (3) (2009) 149–161.
- [14] J. Yuh, T. Young, Dynamic modeling of an axially moving beam in rotation: simulation and experiment, *J. Dyn. Sys. Meas. Control* 113 (1) (1991) 34–40.
- [15] B.O. Al-Bedoor, Y.A. Khulief, Vibrational motion of an elastic beam with prismatic and revolute joints, *J. Sound. Vib.* 190 (2) (1996) 195–206.
- [16] A.A. Shabana, R.Y. Yakoub, Three dimensional absolute nodal coordinate formulation for beam elements: theory, *J. Mech. Des.* 123 (4) (2001) 606–613.
- [17] J. Gerstmayr, H. Sugiyama, A. Mikkola, Review on the absolute nodal coordinate formulation for large deformation analysis of multibody systems, *J. Comput. Nonlin. Dyn.* 8 (3) (2013), 031016.
- [18] A. Olshevskii, O. Dmitrochenko, H.I. Yang, C.W. Kim, Absolute nodal coordinate formulation of tetrahedral solid element, *Nonlinear Dyn.* (2017).
- [19] P. Li, C. Liu, Q. Tian, H. Hu, Y. Song, Dynamics of a deployable mesh reflector of satellite antenna: parallel computation and deployment simulation, *J. Comput. Nonlin. Dyn.* 11 (6) (2016), 061005.
- [20] M. Shan, J. Guo, E. Gill, Deployment dynamics of tethered-net for space debris removal, *Acta Astronaut.* 132 (2017) 293–302.
- [21] Z. Shen, Q. Tian, X. Liu, G. Hu, Thermally induced vibrations of flexible beams using absolute nodal coordinate formulation, *Aerosp. Sci. Technol.* 29 (1) (2013) 386–393.
- [22] K. Kawaguti, Y. Terumichi, S. Takehara, S. Kaczmarczyk, K. Sogabe, The study of the tether motion with time-varying length using the absolute nodal coordinate formulation with multiple nonlinear time scales, *J. Syst. Des. Dyn.* 1 (3) (2007) 491–500.
- [23] J.L. Tang, G.X. Ren, W.D. Zhu, H. Ren, Dynamics of variable-length tethers with application to tethered satellite deployment, *Commun. Nonlinear Sci. Numer. Simul.* 16 (8) (2011) 3411–3424.
- [24] D. Garcia-Vallejo, J.L. Escalona, J. Mayo, J. Dominguez, Describing rigid-flexible multibody systems using absolute coordinates, *Nonlinear Dyn.* 34 (2003) 75–94.
- [25] M. Arnold, O. Brülls, Convergence of the generalized- $\alpha$  scheme for constrained mechanical systems, *Multibody Syst. Dyn.* 18 (2007) 185–202.
- [26] J.G. De Jalon, E. Bayo, *Kinematic and Dynamic Simulation of Multibody Systems: the Real-time Challenge*, Springer Science & Business Media, 2012.
- [27] A.A. Shabana, *Dynamics of Multibody Systems*, Cambridge University Press, 2013.
- [28] K. Nachbagauer, P. Gruber, J. Gerstmayr, Structural and continuum mechanics approaches for a 3D shear deformable ANCF beam finite element: application to static and linearized dynamic examples, *J. Comput. Nonlin. Dyn.* 8 (2) (2013), 021004.
- [29] M. Xue, Y. Ding, Two kinds of tube elements for transient thermal-structural analysis of large space structures, *Int. J. Numer. Meth. Eng.* 59 (2004).
- [30] K.H. Huebner, E.A. Thornton, *The Finite Element Method for Engineers*, John Wiley & Sons, 1982.